Identification of Na+/H+ exchange as a new target for toxic polycyclic aromatic hydrocarbons.

Laurence Huc, Lydie Sparfel, Mary Rissel, Marie-Thérèse Dimanche-Boitre, André Guillouzo, Olivier Fardel, Dominique Lagadic-Gossmann

The FASEB Journal express article 10.1096/fj.03-0316fje. Published online December 4, 2003.

Identification of Na^+/H^+ exchange as a new target for toxic polycyclic aromatic hydrocarbons in liver cells

Laurence Huc, Lydie Sparfel, Mary Rissel, Marie-Thérèse Dimanche-Boitrel, André Guillouzo, Olivier Fardel, and Dominique Lagadic-Gossmann

INSERM U456, Détoxication et Réparation Tissulaire, Faculté de Pharmacie, Univ. Rennes 1, 2 av du Professeur Léon Bernard, 35043 RENNES Cedex, FRANCE

Corresponding author: Dr. Dominique Lagadic-Gossmann, INSERM U456, Faculté de Pharmacie Université Rennes 1, 2, avenue du Professeur Léon Bernard 35043 RENNES cedex, France. E-mail: Dominique.Lagadic@rennes.inserm.fr

ABSTRACT

The ubiquitous environmental pollutants polycyclic aromatic hydrocarbons are responsible for important carcinogenic and apoptotic effects, whose mechanisms are still poorly understood, owing to the multiplicity of possible cellular targets. Among these mechanisms, alterations of ionic homeostasis have been suggested. In this work, the effects of benzo(a)pyrene [B(a)P] on pH_i were tested in the rat liver F258 epithelial cell line, using the fluoroprobe carboxy-SNARF-1. After a 48-h treatment, B(a)P (50 nM) induced an alkalinization, followed by an acidification after 72 h and the development of apoptosis. Determinations of pH_i recovery following an acid load showed an increased acid efflux at 48 h. Cariporide inhibited both the early alkalinization and the increased acid efflux, thus suggesting the involvement of Na^+/H^+ exchanger 1 (NHE1). Besides, α-naphtoflavone (α-NF), an inhibitor of CYP1A1-mediated B(a)P metabolism, prevented all pH_i changes, and NHE1 activation was blocked by the antioxidant thiourea, which inhibited CYP1A1 metabolism-dependent H_2O_2 production. Regarding B(a)P-induced apoptosis, this was prevented by α-NF and bongkrekic acid, an inhibitor of mitochondria-dependent apoptosis. Interestingly, apoptosis was significantly reduced by cariporide. Taken together, our results indicate that B(a)P, via H_2O_2 produced by CYP1A1-dependent metabolism, induces an early activation of NHE1, resulting in alkalinization; this appears to play a significant role in mitochondria-dependent B(a)P-induced apoptosis.

Key words: intracellular pH • benzo(a)pyrene • apoptosis • metabolism

Polycyclic aromatic hydrocarbons (PAHs), such as benzo(a)pyrene [B(a)P], are ubiquitous environmental pollutants notably formed during the burning of fossil fuels and cigarette smoking products (e.g., tobacco) or during cooking and to which humans are commonly exposed (1). Due to their high lipophilicity, they can easily enter cells, where they are usually metabolized into reactive metabolites by xenobiotic metabolizing enzymes, especially cytochrome P450 1A1. Note that the produced metabolites include the formation of proposed electrophilic ultimate intermediates, such as the B(a)P 7,8 diol- 9,10 epoxide, which has been shown to form mutagenic DNA adducts in various target organs (2).

Partly on the basis of the genotoxic properties described above, PAHs are now recognized to be complete carcinogens exhibiting both tumor-initiating and tumor-promoting properties (3). In addition to these carcinogenic properties, PAHs may also exert major immunosuppressive effects (4–7) and possible effects on, for example, the endocrine system (8) and the cardiovascular system (9). In vitro exposure to PAHs also results in major toxicity in some cell types, especially through induction of cell cycle alteration, oxidative damage, or apoptosis. For example, B(a)P has been shown to trigger apoptosis in cultured liver cells as well as in progenitor B cells and oocytes (10) and to decrease growth of isolated lymphocytes (11).

The aryl hydrocarbon receptor (AhR), a ligand-activated transcription factor of the basic helix-loop-helix family, is considered to play a major role in many toxic effects due to PAHs. It displays high affinity binding to various PAHs and, upon activation by these compounds, can act on transcription of various PAH-responsive genes. Thus, CYP1A1 is usually markedly up-regulated in an AhR-dependent manner by PAHs, resulting in an increased formation of mutagenic and toxic metabolites of PAHs. AhR-unrelated mechanisms may however also account for some properties of PAHs (12).

Regarding molecular events underlying PAH toxicity, several studies have implied protein kinases (p38, c-jun NH2-terminal kinase 1 JNK), proteins of the Bcl-2 family, and caspases to be important elements of the PAH-induced apoptotic cascade (10, 13, 14). However, early cellular signaling pathways responsible for the AhR-dependent and -independent toxicity of PAHs remain largely unknown. Depending on the concentration and the experimental system used, they might involve multiple and various cellular targets such as mechanisms implicated in the regulation of intracellular ionic concentrations. Indeed, works by Pessah et al. (15) have demonstrated that B(a)P metabolites alter ryanodine receptor function, thereby modulating Ca^{2+} transport across microsomal membrane. Interestingly, studies dealing with intracellular Ca^{2+} have further shown that an early increase of intracellular Ca^{2+} concentration is associated with the tumor-promoting effect of PAHs in human mammary epithelial cells (16) or with immunotoxicity of B(a)P metabolites in human B cells (17). Although calcium might represent one important determinant of PAH toxicity, a role for other ions cannot be excluded yet.

In the present study, we focused on cellular H^+ homeostasis, that is, pH_i regulation, in response to PAHs, because (i) some crosstalks between Ca^{2+} and H^+ regulatory pathways have been previously described (18) and because (ii) cellular H^+ concentrations, notably through Na^+/H^+ exchange 1 (NHE1) modulation, are affected by or affect several situations that also deal with PAHs such as apoptosis, cell growth, lymphocyte activation, and neoplastic transformation (19–22). Thus, NHE1 was described to be activated or inhibited during apoptosis, leading to alkalinization or acidification, respectively (23, 24). Using the rat liver F258 epithelial cell line known to be sensitive to PAHs (25), we provide evidence that acute exposure to PAHs such as B(a)P induces a biphasic variation of pH_i through alterations of NHE1 activity, therefore pointing to intracellular H^+ homeostasis as a new cellular PAH target. Moreover, we show that these PAH-dependent pH_i changes require CYP1A1 activity and related reactive oxygen species (ROS) and are likely involved in and/or reflect induction of apoptosis in F258 cells, thus linking pH_i regulation and toxicity due to PAHs.

MATERIALS AND METHODS

Chemicals

B(a)P, α-naphtoflavone (α-NF), dimethylbenz(a)anthracene (DMBA), benzanthracene (BA), and bongkrekic acid (BgA) were purchased from Sigma (St Louis, MO). 2,3,7,8-Tetrachlorodibenzo-*p*-dioxin (TCDD) was obtained from Cambridge Isotope Laboratories (Cambridge, MA). Thiourea was purchased from Prolabo (Saint Herblain, France). Cariporide was a kind gift from Aventis (Francfort, Germany). All these products were used as a stock solution in dimethyl sulfoxide (DMSO); final concentration of this vehicule in culture medium was <0.05% (v/v), and control cultures received the same concentration of vehicle as treated cultures. Hoechst 33342, dihydroethidine (DHE), and dichlorodihydrofluorescein diacetate (H_2-DCF-DA) were purchased from Molecular Probes (Eugene, OR). DEVD-AMC (Asp-Glu-Asp-7-amino-4-methylcoumarin) was purchased from Bachem (Voisins, France) and Z-Asp-2,6-dichlorobenzoyloxymethyl-ketone (Z-Asp) from Alexis (Lausanne, Switzerland).

Cell culture

The F258 rat liver epithelial cell line was cultured in Williams' E medium supplemented with 10% fetal calf serum, 2 mM L-glutamine, 5 UI/mL penicillin, and 0.5 mg/ml streptomycin at 37°C under a 5% CO_2 atmosphere as described previously (25). Cells were passaged every week using 0.1% trypsin-EDTA solution. F258 cells, growing in exponential phase, were treated 24 h following seeding (at 2.5×10^3 cells/cm^2) with B(a)P and/or the different inhibitors tested (applied to cells 2 h before PAH exposure) for various treatment times. In control cells, confluence was observed only at day 5 after seeding.

Experimental solutions

HCO_3^--buffered solution contained (in mM): NaCl 111.8, KCl 4.7, $MgCl_2$ 1.0, KH_2PO_4 1.2, $CaCl_2$ 1.0, glucose 10.0, and $NaHCO_3$ 23.0, pH adjusted to 7.4 at 37°C using 5% CO_2/95% O_2. HEPES-buffered solution contained (in mM): NaCl 134.8, KCl 4.7, $MgCl_2$ 1.0, KH_2PO_4 1.2, $CaCl_2$ 1.0, glucose 10.0, and HEPES (N-2-hydroxyethylpiperazine-N'-2-ethanesulphonic acid) 10, pH adjusted to 7.4 at 37°C with NaOH. In Na^+-free medium, NaCl was replaced with 134.8 mM choline, and the pH was adjusted to 7.4 at 37°C with KOH. When ammonium chloride (NH_4Cl 20 mM; Sigma) was used, 20 mM NaCl were removed from the medium to avoid any change of osmotic force. NH_4Cl was added to solutions shortly before use. We added and then removed NH_4Cl to induce an acid load in order to activate the pH_i-regulatory mechanisms (26). Cariporide (30 μM) (a known inhibitor of Na^+/H^+ exchange isoform 1) was added to solution shortly before use. Nigericin (Sigma) calibration solutions used in this study have been described elsewhere (27).

Measurement of pH_i

The pH_i of F258 cells cultured on glass coverslips was monitored using the pH-sensitive fluorescent probe carboxy-SNARF-1 (carboxy-seminaphtorhodafluor; Molecular Probes) (28). Cells were loaded with SNARF by incubating them in a 5 μM solution of the acetoxy-methyl ester for 20 min at 37°C, just before performing the pH_i recording. SNARF-loaded cells were

placed in a continuously perfused recording chamber (at a temperature of 36±1°C) mounted on the stage of an epifluorescent microscope (Nikon Diaphot). F258 cells were then excited with light at 514 nm, and fluorescence from the trapped probe was measured at 590 and 640 nm. The necessary setup to produce and detect the fluorescence has been described previously (29). Emitted fluorescence signals were recorded every 12 s and originated from a small area of coverslip representing ~10 cells in the field of view. All the selected cells exhibited an intact plasma membrane, which is an absolute requirement when performing pH_i measurements using carboxy-SNARF-1; that is why a sufficient SNARF loading was always looked for before the experiment, as estimated by the intensity of the fluorescence light emitted. The emission ratio 640/590 (corrected for background fluorescence) detected from intracellular SNARF was calculated and converted to a linear pH scale using in situ calibration obtained by nigericin technique described elsewhere (28). In the set of experiments aimed at validating the concentration-dependent kinetic effects of B(a)P, about 12 measurements per coverslip (10 coverslips tested in each case) were carried out in order to estimate the percentage of pH_i measurements given similar values.

Estimation of intracellular intrinsic buffering power at different pH_i

The method used to estimate intracellular intrinsic buffering power (β_i) has been described previously (27). In brief, a stepwise reduction of external NH_4Cl (from 20 mM) was applied to selected cells. Each reduction in NH_4^+ resulted in the generation of intracellular H^+, due to the dissociation of NH_4^+ into H^+ ions and NH_3, with subsequent efflux of NH_3. The resultant changes (Δ) in pH_i were used to estimate β_i as follows: $\beta_i = \Delta[NH_4^+]_i/\Delta pH_i$, where $[NH_4^+]_i = [NH_4^+]_e \times 10^{(pHi-pHe)}$. In this latter equation, $[NH_4^+]_i$ and $[NH_4^+]_e$ were intracellular and extracellular ammonium ion concentrations, respectively; pH_i and pH_e were intracellular and extracellular pH, respectively. The experiments were carried out in the absence of extracellular Na^+ in order to prevent acid extrusion and in the presence of barium (1 mM) to reduce NH_4^+ efflux through potassium channels (30).

Calculation of sarcolemmal acid efflux

Details of the method for calculating acid efflux (J^e_H) during pH_i recovery in cells have been described previously (27). In brief, acid efflux was estimated using the following equation: $J^e_H = \beta_T \times dpH_i/dt$, where β_T is the total intracellular buffering power and dpH_i/dt is the rate of pH_i recovery at any given pH_i. In HEPES-buffered medium, β_T equals the intrinsic buffering power β_i. In the present study, when effects of B(a)P treatments on J^e_H were studied, we used the constant value β_i given in the Results, because we found that β_i was insensitive to pH_i under such conditions. Following determinations of the pH_i dependence of acid effluxes from control and B(a)P-treated cells, the kinetic enzymatic parameters (V_{max}, $K'_{[H^+]}$) of a data fit curve realized according to an allosteric model were estimated using a computer program designed for nonlinear regression data analysis (GraphPad Software, Prism 3.02).

Microscopical detection of apoptosis

Microscopical detection of apoptosis was performed in both floating and adherent cells, using Hoechst 33342 labeling. In brief, culture media and trypsinized-adherent cells were collected and then washed with phosphate-buffered saline (PBS), stained with Hoechst 33342 (0.5 μg/ml) in

PBS, and inspected using a fluorescence Olympus BX60 microscope. Cells with apoptotic nuclei, that is, condensed or fragmented, were then counted, in comparison with total population (n>200 nuclei).

Caspase activity assay

Caspase activity assay has been described previously (31). In brief, F258 cells were lysed in the caspase activity buffer. Crude cell lysates (40 μg) were incubated with 80 μM DEVD-AMC for 2 h at 37°C. Caspase-mediated cleavage of DEVD-AMC was measured by spectrofluorimetry (Spectromax Gemini, Molecular Devices) at the excitation/emission wavelength pair of 380/440 nm. The caspase activity was given in % of fluorescence arbitrary units compared with control.

Membrane isolation and Western blotting

Following treatments, cells were harvested, washed with PBS, collected, and placed in a buffer containing 120 mM NaCl, 10 mM Tris, pH 7.4, 0.1 mM PMSF, 0.1 mM benzamidine, 37.5 μM ALLN (calpain I inhibitor), and a proteinase inhibitor cocktail. Samples were homogenized at 4°C for 30 s, incubated on ice for 30 s, and then homogenized again for 30 s with mechanical homogenizer. To obtain crude membrane fractions, we subjected homogenates to a series of centrifugation steps as described previously (32). Total protein was quantitated using the Bio-Rad (Hercules, CA) protein assay kit. Samples were heated for 5 min at 37°C and then analyzed by 9% SDS-PAGE and blotted onto nitrocellulose membranes. In brief, nitrocellulose membranes were incubated first in 10% Tris-buffered solution (TBS) and milk overnight at 4°C and then with primary antibody anti-NHE1 (N1P1) raised against a fusion protein encoding the last 157 amino acids of the human NHE1 C terminus (kindly given by Josette Noël, Montréal, Canada) diluted in TBS overnight, at 4°C, with constant rocking on a shaker. After three washes with TBS, the blots were incubated with horseradish peroxidase-conjugated secondary goat vs. rabbit antibody at room temperature. Revelation was performed by chemiluminescence. Densitometry data analysis was performed using the software Bio-Profil Bio1D (Vilber-Lourmat, France); to normalize the NHE1 signals, we used β-catenin (mouse monoclonal antibody, sc-7963, Santa Cruz Biotechnology, Santa Cruz, CA) as an invariant protein marker.

Reactive oxygen species (ROS) detection

Production of ROS was assessed fluorometrically using oxidation-sensitive fluorescent probes H_2-DCF-DA and DHE to detect H_2O_2 and $O_2^{\cdot-}$, respectively. F258 cells were pretreated with α-NF, thiourea, or vehicule and H_2-DCF-DA (1 μM) or DHE (5 μM) for 2 h, and then B(a)P was added. After a 24-h treatment, cells were collected and samples analyzed using a FACSCalibur flow cytometer (Becton-Dickinson, Franklin Lakes, NJ). Fluorescence emission from oxidized H_2-DCF-DA was detected at 525 nm and oxidized DHE at 605 nm. Prooxidants were used as positive controls: H_2O_2 (10 mM) for H_2-DCF-DA and menadione (100 μM) for DHE. Each measurement was conducted on 10,000 cells and analyzed on Cell Quest software (Becton-Dickinson). Four independent experiments were carried out.

Statistical analysis

All data are quoted as mean ± SE along with number of observations (*n*) corresponding, if not otherwise stated, to the number of separate cultures used. ANOVA followed by Newman-Keuls test was used to test the effects of B(a)P. Differences were considered significant at the level of $P<0.05$. Statistical analysis using a one-way ANOVA was performed to test whether there were differences in the estimated values of V_{max} and $K'_{[H^+]}$ between control and treated groups.

RESULTS

Effects of PAHs on pH_i of F258 cells

In the first set of experiments, we tested the effects of a low dose (50 nM) and a high dose (5 µM) of B(a)P on resting pH_i in F258 cells following various times of treatment, in the presence of HEPES-buffered medium (Fig. 1*A*). Whereas no effect of B(a)P was detected upon an acute exposure (<1 h) with 5 µM or 50 nM (data not shown), we have found that using 50 nM B(a)P, a significant alkalinization was induced after 48 h when compared with untreated cells, followed by an acidification after a 72-h and 96-h treatment. Such pH_i alterations were also detected when a more physiological buffer (HCO_3^-/CO_2) was used in the extracellular medium (Fig. 1*B*). Similar biphasic variations also occurred in 5 µM B(a)P-treated cells but were detected earlier. Indeed, alkalinization developed after a 12-h treatment, whereas no variation was observed following a 24-h treatment with the low dose. Experiments performed to test the number of cells recruited for alkalinization at 12 h for 5 µM B(a)P and at 48 h for 50 nM B(a)P (i.e., at the times alkalinization was detected) pointed to a very probable dose-dependent kinetic effect of this PAH on pH_i because, in both cases, ~80% of pH_i measurements gave an alkaline shift of similar amplitude (data not shown).

In an attempt to elucidate the systems responsible for such pH_i changes, we measured the rate of pH_i recovery following an acid load induced by an NH_4^+ prepulse, in F258 cells treated or not with 50 nM or 5 µM B(a)P. As shown in Figure 2*A* and 2*B*, the rate of pH_i recovery was markedly increased after a 48-h exposure to 50 nM B(a)P; similar results were obtained after a 12-h exposure to 5 µM B(a)P (data not shown). Such an increase might be due either to a decrease of the intrinsic buffering power (β_i) or an increase of H^+-equivalent extrusion. Estimations of β_i in F258 cells showed that this parameter was unchanged by treatment with B(a)P, whatever the concentration and the time of treatment, and gave a mean β_i value of 13.13 ± 4.03 mM (n=113 estimations from 53 coverslips), which was not dependent on pH_i (data not shown). Estimations of the mean H^+-equivalent efflux, J_e^H ($dpH_i/dt \times \beta_i$), at a pH_i of 6.9 following various times of B(a)P treatment clearly indicated an increase of the acid extrusion at 48 h and moreover showed that this up-regulation progressively returned toward control values after 72 h (Fig. 2*C*). In another set of experiments, we verified that the rate of background acid loading in F258 cells, that is, the loading detected when inhibiting pH_i-regulating mechanisms operative in HEPES-buffered solution (a Na^+-free solution was then used) remained unchanged upon treatments with B(a)P (data not shown). Taken together, these data point to the activation of one or several alkalinizing transporter systems that might be responsible for both the transient alkalinization and the transient increase of acid efflux.

To identify the alkalinizing transporter responsible for the effects of B(a)P on H^+ homeostasis described above, we tested the involvement of the Na^+/H^+ exchanger 1, because in HEPES-buffered medium, this transporter has been shown to carry most of acid extrusion, all HCO_3^--dependent systems being inhibited (27). The following experiments demonstrated the constitutive presence of NHE activity in untreated F258 cells. Indeed, pH_i recovery following the acid load was found to be strongly inhibited upon removal of extracellular Na^+; moreover, upon readdition of extracellular Na^+, acid extrusion was rapidly reactivated (data not shown). The use of the NHE1-specific inhibitor cariporide (30 μM) (33) allowed us to identify the Na^+-dependent transporter as the isoform 1 of NHE (Fig. 3*B*).

We next tested the role of NHE1 in the alkalinization recorded after a 48-h treatment with 50 nM B(a)P. This concentration was chosen because it is possibly encountered in the environment. Cotreatments with 50 nM of B(a)P and 30 μM of cariporide were thus performed. As illustrated in Figure 3*A*, measurements of resting pH_i after a 48-h exposure showed an inhibition of B(a)P-induced alkalinization, as well as acidification, under such conditions. After an acid load induced by NH_4^+ removal, the presence of cariporide significantly blocked pH_i recovery in B(a)P-treated cells (Fig. 3*C*) similarly to what occurred in control cells (Fig. 3*B*). Taken together, these results pointed to NHE1 as the B(a)P- activated alkalinizing system responsible for the intracellular alkalinization measured after a 48-h treatment.

Role of CYP1A1-dependent metabolism and related ROS production in pH_i variations

The direct involvement of AhR was analyzed by exposing F258 cells to TCDD (50 nM), which binds to AhR without being metabolized by CYP1A1 (34). Measurements of pH_i were performed following 48 and 72 h of treatment and showed no effect of this molecule (Fig. 4*A*). Similar results were obtained with BA (50 nM), whereas DMBA (50 nM) induced both an alkalinization at 48 h (ΔpH_i =+0.125±0.05, n=11) and an acidification at 72 h (ΔpH_i=–0.150±0.05, n=10).

To test the involvement of B(a)P metabolism through CYP1A1 in pH_i variations, we next cotreated F258 cells with 50 nM B(a)P and 10 μM α-NF, known as a CYP1A1 and AhR antagonist (35), and then measured resting pH_i following 48 h and 72 h of treatment. As shown in Figure 4*B*, both the alkalinization at 48 h and the acidification at 72 h were prevented under such conditions.

In Figure 5, we tested the effects of α-NF on the up-regulation by B(a)P of the acid efflux. Similar to what was observed with resting pH_i, Figure 5*A* clearly shows that in the presence of α-NF, B(a)P (50 nM) was no longer capable of up-regulating acid extrusion, which was confirmed when determining the mean pH_i dependence of J^e_H from several experiments (Fig. 5*B*). Taken together, these results confirm the crucial involvement of CYP1A1-dependent metabolism in the activation of NHE1 by B(a)P.

To determine the level of NHE1 regulation by B(a)P, we carried out kinetic analysis of the exchanger activity following 48 h of treatment. In Figure 6*A*, no significant change in V_{max} was observed, whereas $K'_{[H^+]i}$ was decreased by half upon B(a)P treatment (control, 65.55±1.57 nM vs. B(a)P, 31.10±7.12 nM; n=7), suggesting that B(a)P modulated Na^+/H^+ exchange activity by increasing its affinity for H^+. The results given in Figure 6*B* point to no change in NHE1 protein

expression by B(a)P. The fact that xenobiotic metabolism can induce a production of ROS such as H_2O_2 and $O_2^{\cdot-}$ and that such species are also known to regulate NHE1 activity (36, 37) prompted us to study ROS production and its impact on NHE1 activation. Figure 7*A* shows that an H_2O_2 (detected by H_2-DCF-DA) rather than an $O_2^{\cdot-}$ production (detected by DHE) occurred following a 24-h treatment with 50 nM B(a)P, that is, before NHE1 activation. This H_2O_2 production was found to be dependent on CYP1A1, since inhibited by 10 μM α-NF. In the presence of the antioxidant molecule thiourea, at a concentration (10 mM) capable of preventing any H_2O_2 production (Fig. 7*A*), no more alkalinization was observed following a 48-h treatment with B(a)P (Fig. 7*B*). Furthermore, thiourea blocked any up-regulation of acid extrusion following B(a)P treatment, as shown in Figure 7*C*. Taken together, these results show that the activity of NHE1 is modulated by B(a)P likely via H_2O_2 produced by CYP1A1-dependent metabolism.

Relationship between PAH-mediated alterations of pH_i and toxicity

PAHs are known to elicit cell death through an apoptotic mode in hepatic cells (10). Therefore, we tested whether the pH_i variations detected in the present study might play a role in the toxic effects of these compounds. We first verified that B(a)P was indeed toxic for F258 cells. Thus, a decrease of cell viability was observed upon B(a)P as estimated by MTT assay (IC_{50}=37.7±16.3 nM after 96-h treatment). As illustrated in Figure 8*A*, B(a)P applied at a concentration of 50 nM for 48 and 72 h was found to increase the number of apoptotic nuclei compared with control conditions, as estimated by chromatin staining with Hoechst 33342. Interestingly, similar results were obtained with DMBA but not with BA (Fig. 8*A*). Moreover, cotreatments of F258 cells with 50 nM of B(a)P (Fig. 8*B*) or DMBA (data not shown) and 10 μM of α-NF prevented any toxicity of these PAHs. This therefore indicates that besides affecting pH_i, metabolites of B(a)P and DMBA are the most likely responsible for induction of apoptosis.

Xenobiotic-induced apoptosis is often reported to be mediated by mitochondria (38) and to be associated with a mitochondria-dependent acidification (39). To test whether similar effects were occurring here, we used BgA, known to inhibit the breakdown of the mitochondrial transmembrane potential (ΔΨm) and hence apoptosis (40). Figure 8*B* shows that BgA markedly reduces the apoptosis percentage, pointing to a role for mitochondria in B(a)P apoptotic signaling. With the aim of testing the possible involvement of mitochondria in pH_i variations, we next measured resting pH_i in cells cotreated with B(a)P and BgA. The results, given in Figure 8*C*, showed that whereas alkalinization was maintained after 48 h of treatment with B(a)P (50 nM), late acidification was prevented, most likely indicating that mitochondria were indeed involved in the development of B(a)P-induced secondary cytosolic acidification.

To analyze the role of NHE1-dependent alkalinization in PAH-induced toxicity, we next cotreated F258 cells with B(a)P or DMBA (50 nM) and cariporide (30 μM) and estimated the number of apoptotic nuclei under such conditions. Figure 9*A* shows that the specific inhibitor of NHE1 significantly reduced toxicity of B(a)P; similar protection was observed for DMBA (data not shown), especially at 72 h (reduction by 36.4% and 34.8%, respectively, compared with control PAH-treated cells; Fig. 9*A*). Furthermore, such a protective effect of cariporide was also detected when cariporide was added 24 h after the onset of PAH treatment (i.e., before alkalinization occurrence) but not when this addition was performed 48 h later (i.e., after alkalinization had developed) (Fig. 9*A*). Figure 9*B* further shows that cariporide also reduced the

caspase activity induced by B(a)P. We have verified that cariporide had no effect on CYP1A1 activity by EROD activity measurements as well as on the production of either B(a)P metabolites or H_2O_2 (unpublished data), therefore ruling out any direct inhibitory action of cariporide on the metabolism of B(a)P. The present results therefore strongly suggest a link between PAH-induced toxicity and NHE1 activation and/or alkalinization detected at 48 h. In this context, we made a hypothesis that late acidification, which occurred after a 72-h treatment, would have been a mere consequence of prior alkalinization and hence of apoptosis signaling. This was the case because under conditions that inhibited alkalinization, we found that late intracellular acidification was significantly inhibited, as stated above (Fig. 4*A*).

DISCUSSION

PAHs are environmental pollutants exhibiting potent carcinogenic and immunotoxic effects. Whereas alterations of Ca^{2+} homeostasis have been shown to be partly responsible for such effects (16), up to now, to our knowledge, no information was available regarding putative effects of PAHs on another biologically important ion, namely H^+. The present work indicates for the first time to the best of our knowledge that PAHs, following oxidative metabolism by CYP1A1, are capable of modifying cellular H^+ homeostasis in liver epithelial cells through alterations of Na^+/H^+ exchanger located at the plasma membrane and following mitochondrial targeting. Moreover, these pH_i changes were shown to be closely associated with the induction of PAH-related toxic effects.

Exposing F258 cells to B(a)P induced biphasic pH_i changes with first an alkalinization followed by an acidification, in both CO_2/HCO_3^-- and HEPES-buffered solutions. Moreover, we observed that the greater the concentration of B(a)P was, the faster pH_i changes appeared. Concerning the early alkalinization, the hypothesis put forward to explain such a pH_i variation was that B(a)P was increasing an acid extrusion pathway. Following acid loads, we found that the resulting pH_i recovery was increased at the times corresponding to pH_i alkaline shift, as compared with control. This up-regulation, however, appeared to be transient because, following longer treatments with B(a)P, no increase in the rate of pH_i recovery was detected. Because the intracellular intrinsic buffering power and the background acid loading (due to acid influx and/or metabolic acid production) remained unchanged upon B(a)P, the present data were therefore in favor of a transient activation by B(a)P of one or several acid extruders in F258 cells.

As pH_i variations were shown as still occurring in the presence of HEPES as extracellular buffer, we next examined whether the ubiquitous Na^+/H^+ exchange 1 (NHE1) might be one such transporter. Using a specific inhibitor of this transporter, we showed that NHE1 was indeed active in F258 cells and that, following 48-h treatments with 50 nM B(a)P, both the alkalinization and the increase of acid extrusion were strongly inhibited. Taken together, the present results demonstrate that upon B(a)P treatment, the activity of NHE1 undergoes two phases: first, an up-regulation, which underlies the increase in resting pH_i, and second, a recovery toward basal level. When seeking the level of B(a)P-induced regulation on NHE1, we found that NHE1 protein expression was unaffected. Moreover, modulation of NHE1 activity seemed to be due to an increase of its H^+ affinity; indeed, $K'_{[H^+]i}$ was diminished by half upon a 48-h treatment with 50 nM B(a)P, without any change in V_{max}, this latter result being in accordance with no change in the NHE1 protein expression level.

Based on the fact that most of the PAH carcinogenic and toxic effects rely on the AhR (41) and that the AhR is expressed in F258 cells (25), its possible involvement in the above alterations of the H^+ homeostasis was tested in this study by using the very potent AhR ligand TCDD. TCDD failed to induce any pH_i change, whereas α-NF—a partial antagonist of this receptor but overall, in the present case, a CYP1A1 metabolism inhibitor (data not shown)—completely prevented the resting pH_i changes as well as the NHE1 up-regulation induced by B(a)P. Taken together, these results therefore suggest that direct activation of AhR is not sufficient for inducing pH_i alterations. It might be argued that, as recently shown for the AhR-driven *Bax* gene expression (14), whereas the B(a)P-activated AhR would be capable of eliciting the presently detected pH_i changes, the TCDD-activated AhR would not, due to different AhR response elements (AHREs) present in the target genes. However, the PAH benzanthracene, which binds AhR and whose metabolism leads to nontoxic products (42), was also found to be ineffective on pH_i, even at a high concentration (5 μM; data not shown). In this context, the inhibitory effects of α-NF strongly point to the involvement of bioreactive PAH metabolites in these alterations. Nevertheless, despite its nondirect implication, AhR very likely contributed in this scheme, due to its determinant role in activating the expression of CYP1A1 gene (43).

Because PAH metabolism appeared to be determinant and considering that very acute treatment (<1 h) with high concentrations of B(a)P (5 and 10 μM) had no effect on pH_i (data not shown), the delay between B(a)P application and the appearance of H^+ homeostasis changes might then be necessary for bioreactive metabolites and ROS to be formed and accumulate inside the cells so as to elicit their effects on pH_i. In support of this hypothesis, we observed that a dose of 5 μM B(a)P elicited an earlier alkalinization compared with 50 nM. With respect to a role for B(a)P metabolites in the present effects, note that a single *o*-quinone metabolite of B(a)P, B(a)P-7,8-dione, has recently been shown to be responsible for time-dependent biphasic alterations in the function of the ryanodine receptor 1 (RyR1), first activating then inhibiting channel activity (15). To explain their results, the authors have then proposed that the activation of RyR1 was due to production of H_2O_2 and the inhibition, to direct binding of metabolites to the protein. This has led us to suppose that B(a)P metabolism was affecting NHE1 activity via ROS production.

We first showed that in B(a)P-treated F258 cells, H_2O_2 production was dependent on CYP1A1 metabolism and occurred before the alkalinization onset. Experiments performed with the antioxidant molecule thiourea further demonstrated the involvement of these ROS in the modulation by B(a)P of NHE1 activity. Concerning a role for H_2O_2 in NHE1 regulation, note that in cardiac cells, treatment with exogenous H_2O_2 has been shown to be capable of stimulating sarcolemmal NHE activity, notably through an increase in phosphorylation of the exchanger by action of diverse protein kinases, including mitogen-activated protein kinases (MAPKs) (44, 45). As PAH metabolism is known to activate the MAPKs c-jun NH2-terminal kinase 1 (JNK) and p38 (10, 46, 47), these might be involved in the transient B(a)P-induced NHE1 up-regulation. This remains to be tested.

As reported above, B(a)P-induced intracellular alkalinization was followed by a significant intracellular acidification. Based on the fact that after longer treatments, the activity of NHE1 did not differ between treated and untreated cells and therefore would not be involved, we tested whether mitochondria might be responsible for this late acid load by using BgA (to target the adenine nucleotide translocase of mitochondria [48]). Our results showed that BgA prevented intracellular acidification without any effect on prior alkalinization, thus indicating that B(a)P

induced late acidification results from an effect on mitochondria. An important observation in this study was that the occurrence of prior alkalinization appeared to be necessary for the acidification to develop, because inhibited by NHE1 inhibitors. Taken together, these results strongly suggest that, regarding the alterations in H^+ homeostasis presently described, metabolism of B(a)P (and probably that of DMBA) essentially targets NHE1 located at the plasma membrane, thus inducing alkalinization, whereas acidification would be a mere consequence of prior NHE1 activation. In this context, due to the presence of other important pH_i-regulating mechanisms in the plasma membrane (eg Na^+-HCO_3^- symport, Cl^-/HCO_3^- inhibited in HEPES-buffered solutions), it might then be possible that B(a)P metabolism would also affect such transporters. This has to be tested yet.

Following demonstration of PAH-induced alterations in H^+ homeostasis in F258 cells, the question remained as to whether these were relevant to the well-known carcinogenic or toxic effects of these chemicals. Indeed, NHE-dependent pH_i change has been shown by several groups to play an important role in proliferating processes (19, 21, 22) as well as in inducing cell death (24, 49, 50), and intracellular acidification is often related to the mitochondrial pathway of apoptosis (51, 52). In our cell model, a B(a)P-induced toxicity was found to be via apoptosis, as already observed in other cell types (10, 53, 54), depending on CYP1A1-related metabolism (since inhibited by α-NF) and mitochondrial dysfunction (since inhibited by BgA). Regarding pH_i, we found that only AhR ligands producing pH_i alterations, that is, B(a)P and DMBA, were capable of inducing cell toxicity, unlike TCDD or BA. Moreover, a high dose of B(a)P (5 μM), which induced fast variations of pH_i, triggered a rapid and massive apoptosis in F258 cells. In this context, the role of pH_i alterations in PAH-induced toxicity was tested by using cariporide to inhibit NHE1-dependent alkalinization.

We found that cotreatment with B(a)P and cariporide significantly reduced toxicity through a specific effect on pH_i. We suppose at this stage that the remaining apoptosis in the presence of cariporide might rely on other pathways, and especially the p53 pathway known to be triggered by the binding of B(a)P-derived reactive metabolites to DNA (55). Taken together, these results are the first to demonstrate the crucial role for NHE1-dependent alkalinization in the development of PAH-induced toxicity (Fig. 10).

According to recent studies, Bax, known to lead to mitochondria dysfunction after translocation, represents one possible target for intracellular alkalinization during apoptotic processes (24, 52, 56). Because a recent study has shown that Bax transcription is increased upon PAH exposure, thereby inducing cell death (14, 57), we might then suppose that the NHE1-dependent alkalinization would create a permissive environment favoring translocation of Bax to mitochondria and hence mitochondrial dysfunction and related cytosolic acidification, all these leading to activation of caspases and ultimately to cell death. Analysis of the precise sequence of events is currently under investigation. Finally, considering the well-described carcinogenic effects of B(a)P (2), the proapoptotic role of NHE1 presently shown might be viewed as possibly affording some protection against neoplastic transformation induced by PAHs, through an elimination process of cells exhibiting DNA attack by reactive metabolites and ROS and hence possible DNA mutations.

In conclusion, the present study demonstrates alterations in H^+ homeostasis upon PAH exposure, which might play a crucial role in the toxic effects induced by these chemicals. Interestingly,

transient activation of NHE1 might constitute an important early signal in the development of the apoptotic cascade induced by toxic chemicals such as PAHs.

ACKNOWLEDGMENTS

This work was supported by grants from the Institut National de Recherche et de Sécurité (INRS) and the Ministère de l'Aménagement du Territoire et de l'Environnement.

REFERENCES

1. Zedeck, M. S. (1980) Polycyclic aromatic hydrocarbons: a review. *J. Environ. Pathol. Toxicol.* **3,** 537–567

2. Pelkonen, O., and Nebert, D. W. (1982) Metabolism of polycyclic aromatic hydrocarbons: etiologic role in carcinogenesis. *Pharmacol. Rev.* **34,** 189–222

3. Ethier, S. P., and Ullrich, R. L. (1982) Induction of mammary tumors in virgin female BALB/c mice by single low doses of 7,12-dimethylbenz[a]anthracene. *J. Natl. Cancer Inst.* **69,** 1199–1203

4. Laupeze, B., Amiot, L., Sparfel, L., Le Ferrec, E., Fauchet, R., and Fardel, O. (2002) Polycyclic aromatic hydrocarbons affect functional differentiation and maturation of human monocyte-derived dendritic cells. *J. Immunol.* **168,** 2652–2658

5. Woods, G. M., Doherty, K. V., Malley, R. C., Rist, M. J., and Muller, H. K. (2000) Carcinogen-modified dendritic cells induce immunosuppression by incomplete T-cell activation resulting from impaired antigen uptake and reduced CD86 expression. *Immunology* **99,** 16–22

6. Burchiel, S. W. (1999) The effects of environmental and other chemicals on the human immune system: the emergence of immunotoxicology. *Clin. Immunol.* **90,** 285–286

7. van Grevenynghe, J., Rion, S., Le Ferrec, E., Le Vee, M., Amiot, L., Fauchet, R., and Fardel, O. (2003) Polycyclic aromatic hydrocarbons inhibit differentiation of human monocytes into macrophages. *J. Immunol.* **170,** 2374–2381

8. Santodonato, J. (1997) Review of the estrogenic and antiestrogenic activity of polycyclic aromatic hydrocarbons: relationship to carcinogenicity. *Chemosphere* **34,** 835–848

9. Mennear, J. H. (1993) Carbon monoxide and cardiovascular disease: an analysis of the weight of evidence. *Regul. Toxicol. Pharmacol.* **17,** 77–84

10. Lei, W., Yu, R., Mandlekar, S., and Kong, A. N. (1998) Induction of apoptosis and activation of interleukin 1beta-converting enzyme/Ced-3 protease (caspase-3) and c-Jun NH2-terminal kinase 1 by benzo(a)pyrene. *Cancer Res.* **58,** 2102–2106

11. Black, K. A., McFarland, R. D., Grisham, J. W., and Smith, G. J. (1989) S-phase block and cell death in human lymphoblasts exposed to benzo[a]pyrene diol epoxide or N-acetoxy-2-acetylaminofluorene. *Toxicol. Appl. Pharmacol.* **97,** 463–472

12. Dertinger, S. D., Lantum, H. B., Silverstone, A. E., and Gasiewicz, T. A. (2000) Effect of 3′-methoxy-4'-nitroflavone on benzo[a]pyrene toxicity. Aryl hydrocarbon receptor-dependent and -independent mechanisms. *Biochem. Pharmacol.* **60,** 189–196

13. Page, T. J., O'Brien, S., Jefcoate, C. R., and Czuprynski, C. J. (2002) 7,12-Dimethylbenz[a]anthracene induces apoptosis in murine pre-B cells through a caspase-8-dependent pathway. *Mol. Pharmacol.* **62,** 313–319

14. Matikainen, T., Perez, G. I., Jurisicova, A., Pru, J. K., Schlezinger, J. J., Ryu, H. Y., Laine, J., Sakai, T., Korsmeyer, S. J., Casper, R. F., et al. (2001) Aromatic hydrocarbon receptor-driven Bax gene expression is required for premature ovarian failure caused by biohazardous environmental chemicals. *Nat. Genet.* **28,** 355–360

15. Pessah, I. N., Beltzner, C., Burchiel, S. W., Sridhar, G., Penning, T., and Feng, W. (2001) A bioactive metabolite of benzo[a]pyrene, benzo[a]pyrene-7,8-dione, selectively alters microsomal Ca2+ transport and ryanodine receptor function. *Mol. Pharmacol.* **59,** 506–513

16. Tannheimer, S. L., Lauer, F. T., Lane, J., and Burchiel, S. W. (1999) Factors influencing elevation of intracellular Ca2+ in the MCF-10A human mammary epithelial cell line by carcinogenic polycyclic aromatic hydrocarbons. *Mol. Carcinog.* **25,** 48–54

17. Mounho, B. J., and Burchiel, S. W. (1998) Alterations in human B cell calcium homeostasis by polycyclic aromatic hydrocarbons: possible associations with cytochrome P450 metabolism and increased protein tyrosine phosphorylation. *Toxicol. Appl. Pharmacol.* **149,** 80–89

18. Vaughan-Jones, R. D., Lederer, W. J., and Eisner, D. A. (1983) Ca2+ ions can affect intracellular pH in mammalian cardiac muscle. *Nature* **301,** 522–524

19. Putney, L. K., Denker, S. P., and Barber, D. L. (2002) The changing face of the Na+/H+ exchanger, NHE1: structure, regulation, and cellular actions. *Annu. Rev. Pharmacol. Toxicol.* **42,** 527–552

20. Benedetti, A., Di Sario, A., Casini, A., Ridolfi, F., Bendia, E., Pigini, P., Tonnini, C., D'Ambrosio, L., Feliciangeli, G., Macarri, G., et al. (2001) Inhibition of the Na(+)/H(+) exchanger reduces rat hepatic stellate cell activity and liver fibrosis: an in vitro and in vivo study. *Gastroenterology* **120,** 545–556

21. Grinstein, S., Smith, J. D., Onizuka, R., Cheung, R. K., Gelfand, E. W., and Benedict, S. (1988) Activation of Na+/H+ exchange and the expression of cellular proto- oncogenes in mitogen- and phorbol ester-treated lymphocytes. *J. Biol. Chem.* **263,** 8658–8665

22. Reshkin, S. J., Bellizzi, A., Caldeira, S., Albarani, V., Malanchi, I., Poignee, M., Alunni-Fabbroni, M., Casavola, V., and Tommasino, M. (2000) Na+/H+ exchanger-dependent

intracellular alkalinization is an early event in malignant transformation and plays an essential role in the development of subsequent transformation-associated phenotypes. *FASEB J.* **14,** 2185–2197

23. Li, J., and Eastman, A. (1995) Apoptosis in an interleukin-2-dependent cytotoxic T lymphocyte cell line is associated with intracellular acidification. Role of the Na(+)/H(+)-antiport. *J. Biol. Chem.* **270,** 3203–3211

24. Khaled, A. R., Moor, A. N., Li, A., Kim, K., Ferris, D. K., Muegge, K., Fisher, R. J., Fliegel, L., and Durum, S. K. (2001) Trophic factor withdrawal: p38 mitogen-activated protein kinase activates NHE1, which induces intracellular alkalinization. *Mol. Cell. Biol.* **21,** 7545–7557

25. Payen, L., Courtois, A., Langouet, S., Guillouzo, A., and Fardel, O. (2001) Unaltered expression of multidrug resistance transporters in polycyclic aromatic hydrocarbon-resistant rat liver cells. *Toxicology* **156,** 109–117

26. Boron, W. F., and De Weer, P. (1976) Intracellular pH transients in squid giant axons caused by CO2, NH3, and metabolic inhibitors. *J. Gen. Physiol.* **67,** 91–112

27. Lagadic-Gossmann, D., Buckler, K. J., and Vaughan-Jones, R. D. (1992) Role of bicarbonate in pH recovery from intracellular acidosis in the guinea-pig ventricular myocyte. *J. Physiol.* **458,** 361–384

28. Buckler, K. J., and Vaughan-Jones, R. D. (1990) Application of a new pH-sensitive fluoroprobe (carboxy-SNARF-1) for intracellular pH measurement in small, isolated cells. *Pflugers Arch.* **417,** 234–239

29. Lagadic-Gossmann, D., Rissel, M., Galisteo, M., and Guillouzo, A. (1999) Intracellular pH alterations induced by tacrine in a rat liver biliary epithelial cell line. *Br. J. Pharmacol.* **128,** 1673–1682

30. Vaughan-Jones, R. D., and Wu, M. L. (1990) Extracellular H+ inactivation of Na(+)-H(+) exchange in the sheep cardiac Purkinje fibre. *J. Physiol.* **428**, 441–466

31. Gilot, D., Loyer, P., Corlu, A., Glaise, D., Lagadic-Gossmann, D., Atfi, A., Morel, F., Ichijo, H., and Guguen-Guillouzo, C. (2002) Liver protection from apoptosis requires both blockage of initiator caspase activities and inhibition of ASK1/JNK pathway via glutathione S- transferase regulation. *J. Biol. Chem.* **277,** 49220–49229

32. Rieder, C. V., and Fliegel, L. (2002) Developmental regulation of Na(+)/H(+) exchanger expression in fetal and neonatal mice. *Am. J. Physiol. Heart Circ. Physiol.* **283,** H273–H283

33. Scholz, W., Albus, U., Lang, H. J., Linz, W., Martorana, P. A., Englert, H. C., and Scholkens, B. A. (1993) Hoe 694, a new Na+/H+ exchange inhibitor and its effects in cardiac ischaemia. *Br. J. Pharmacol.* **109,** 562–568

34. Wilson, C. L., and Safe, S. (1998) Mechanisms of ligand-induced aryl hydrocarbon receptor-mediated biochemical and toxic responses. *Toxicol. Pathol.* **26,** 657–671

35. Sparfel, L., Loewert, M., Huc, L., Payen, L., Guillouzo, A., Lagadic-Gossmann, D., and Fardel, O. (2002) Acute cytotoxicity of the chemical carcinogen 2-acetylaminofluorene in cultured rat liver epithelial cells. *Toxicol. Lett.* **129,** 245–254

36. Rothstein, E. C., Byron, K. L., Reed, R. E., Fliegel, L., and Lucchesi, P. A. (2002) H(2)O(2)-induced Ca(2+) overload in NRVM involves ERK1/2 MAP kinases: role for an NHE-1-dependent pathway. *Am. J. Physiol. Heart Circ. Physiol.* **283,** H598–H605

37. Flowers, L., Bleczinski, W. F., Burczynski, M. E., Harvey, R. G., and Penning, T. M. (1996) Disposition and biological activity of benzo[a]pyrene-7,8-dione. A genotoxic metabolite generated by dihydrodiol dehydrogenase. *Biochemistry* **35,** 13664–13672

38. Robertson, J. D., and Orrenius, S. (2000) Molecular mechanisms of apoptosis induced by cytotoxic chemicals. *Crit. Rev. Toxicol.* **30,** 609–627

39. Matsuyama, S., and Reed, J. C. (2000) Mitochondria-dependent apoptosis and cellular pH regulation. *Cell Death Differ.* **7,** 1155–1165

40. Henderson, P. J., and Lardy, H. A. (1970) Bongkrekic acid. An inhibitor of the adenine nucleotide translocase of mitochondria. *J. Biol. Chem.* **245,** 1319–1326

41. Delescluse, C., Lemaire, G., de Sousa, G., and Rahmani, R. (2000) Is CYP1A1 induction always related to AHR signaling pathway? *Toxicology* **153,** 73–82

42. Lewis, D. F., and Parke, D. V. (1995) The genotoxicity of benzanthracenes: a quantitative structure-activity study. *Mutat. Res.* **328,** 207–214

43. Dertinger, S. D., Nazarenko, D. A., Silverstone, A. E., and Gasiewicz, T. A. (2001) Aryl hydrocarbon receptor signaling plays a significant role in mediating benzo[a]pyrene- and cigarette smoke condensate-induced cytogenetic damage in vivo. *Carcinogenesis* **22,** 171–177

44. Wei, S., Rothstein, E. C., Fliegel, L., Dell'Italia, L. J., and Lucchesi, P. A. (2001) Differential MAP kinase activation and Na(+)/H(+) exchanger phosphorylation by H(2)O(2) in rat cardiac myocytes. *Am. J. Physiol. Cell Physiol.* **281,** C1542–C1550

45. Snabaitis, A. K., Hearse, D. J., and Avkiran, M. (2002) Regulation of sarcolemmal Na(+)/H(+) exchange by hydrogen peroxide in adult rat ventricular myocytes. *Cardiovasc. Res.* **53,** 470–480

46. Yoshii, S., Tanaka, M., Otsuki, Y., Fujiyama, T., Kataoka, H., Arai, H., Hanai, H., and Sugimura, H. (2001) Involvement of alpha-PAK-interacting exchange factor in the PAK1-c-Jun NH(2)-terminal kinase 1 activation and apoptosis induced by benzo[a]pyrene. *Mol. Cell. Biol.* **21,** 6796–6807

47. Kwon, Y. W., Ueda, S., Ueno, M., Yodoi, J., and Masutani, H. (2002) Mechanism of p53-dependent apoptosis induced by 3-methylcholanthrene: involvement of p53 phosphorylation and p38 MAPK. *J. Biol. Chem.* **277,** 1837–1844

48. Scarlett, J. L., Sheard, P. W., Hughes, G., Ledgerwood, E. C., Ku, H. H., and Murphy, M. P. (2000) Changes in mitochondrial membrane potential during staurosporine- induced apoptosis in Jurkat cells. *FEBS Lett.* **475,** 267–272

49. Barriere, H., Poujeol, C., Tauc, M., Blasi, J. M., Counillon, L., and Poujeol, P. (2001) CFTR modulates programmed cell death by decreasing intracellular pH in Chinese hamster lung fibroblasts. *Am. J. Physiol. Cell Physiol.* **281,** C810–C824

50. Rich, I. N., Worthington-White, D., Garden, O. A., and Musk, P. (2000) Apoptosis of leukemic cells accompanies reduction in intracellular pH after targeted inhibition of the Na(+)/H(+) exchanger. *Blood* **95,** 1427–1434

51. Hirpara, J. L., Clement, M. V., and Pervaiz, S. (2001) Intracellular acidification triggered by mitochondrial-derived hydrogen peroxide is an effector mechanism for drug-induced apoptosis in tumor cells. *J. Biol. Chem.* **276,** 514–521

52. Matsuyama, S., Llopis, J., Deveraux, Q. L., Tsien, R. Y., and Reed, J. C. (2000) Changes in intramitochondrial and cytosolic pH: early events that modulate caspase activation during apoptosis. *Nat. Cell Biol.* **2,** 318–325

53. Revel, A., Raanani, H., Younglai, E., Xu, J., Han, R., Savouret, J. F., and Casper, R. F. (2001) Resveratrol, a natural aryl hydrocarbon receptor antagonist, protects sperm from DNA damage and apoptosis caused by benzo(a)pyrene. *Reprod. Toxicol.* **15,** 479–486

54. Chin, B. Y., Choi, M. E., Burdick, M. D., Strieter, R. M., Risby, T. H., and Choi, A. M. (1998) Induction of apoptosis by particulate matter: role of TNF-alpha and MAPK. *Am. J. Physiol.* **275,** L942–L949

55. Wu, J., Gu, L., Wang, H., Geacintov, N. E., and Li, G. M. (1999) Mismatch repair processing of carcinogen-DNA adducts triggers apoptosis. *Mol. Cell. Biol.* **19,** 8292–8301

56. Khaled, A. R., Kim, K., Hofmeister, R., Muegge, K., and Durum, S. K. (1999) Withdrawal of IL-7 induces Bax translocation from cytosol to mitochondria through a rise in intracellular pH. *Proc. Natl. Acad. Sci. USA* **96,** 14476–14481

57. Matikainen, T. M., Moriyama, T., Morita, Y., Perez, G. I., Korsmeyer, S. J., Sherr, D. H., and Tilly, J. L. (2002) Ligand activation of the aromatic hydrocarbon receptor transcription factor drives Bax-dependent apoptosis in developing fetal ovarian germ cells. *Endocrinology* **143,** 615–620

Received April 29, 2003; accepted October 21, 2003.

Fig. 1

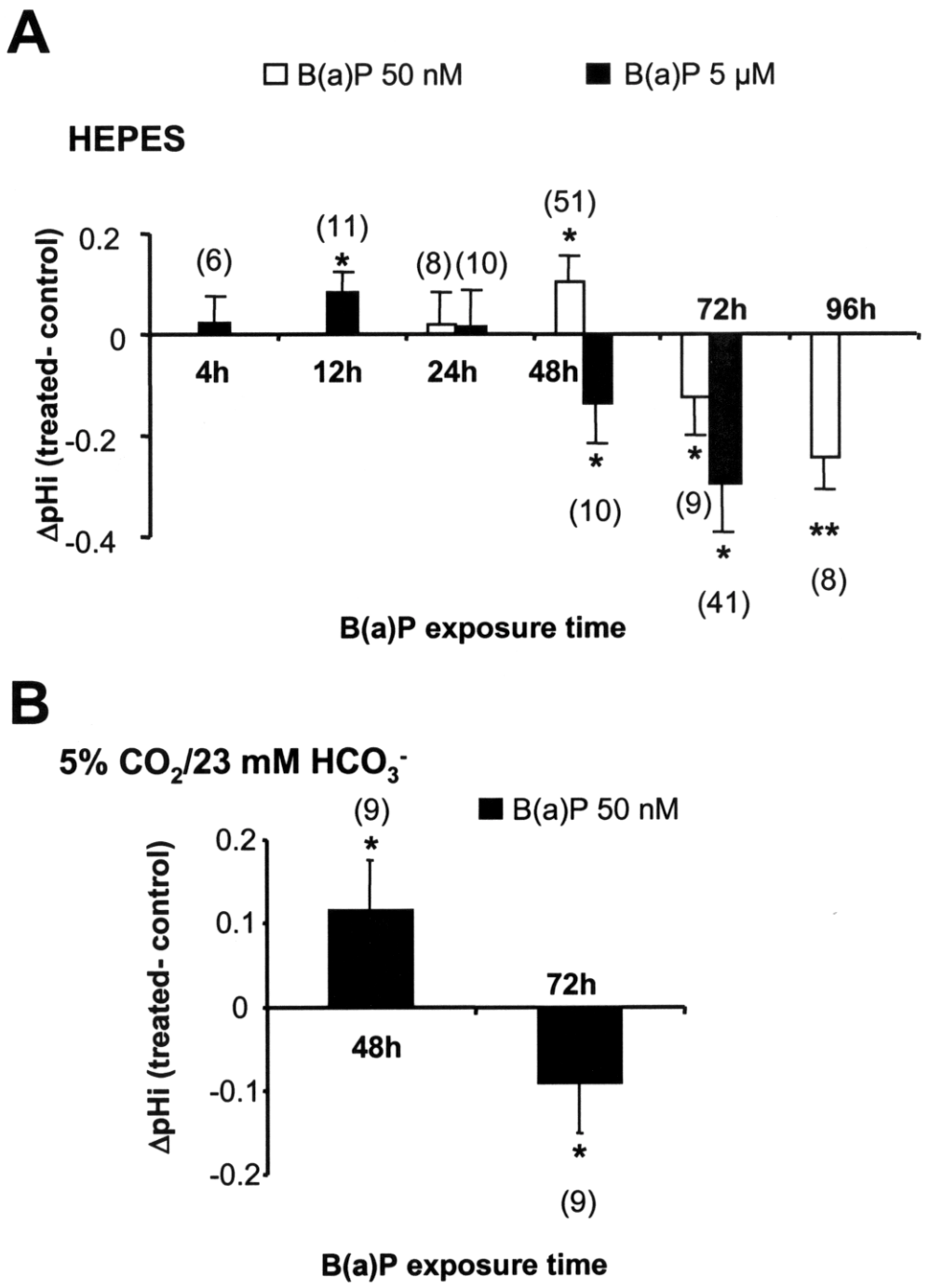

Figure 1. pH_i variations following B(a)P exposure. F258 cells were treated with 50 nM or 5 µM B(a)P for the different times indicated in the graphs. Resting pH_i measurements were monitored by microspectrofluorimetry using the pH-sensitive fluorescent probe, carboxy-SNARF-1. Cells were superfused with HEPES-buffered medium (***A***) or 5% CO_2/23 mM HCO_3^--buffered medium (***B***) (extracellular pH of 7.4 in both conditions). pH_i values were derived from a pH calibration curve (as described in Materials and Methods), and ΔpH_i were calculated by substracting pH_i values in untreated cells from those in treated cells. *$P < 0.05$, **$P < 0.01$. Number in brackets given next to each bar represents the number of coverslips used (i.e., the number of performed measurements) from at least 3 independent experiments. Mean values correspond to the average of all pH_i determinations.

Fig. 2

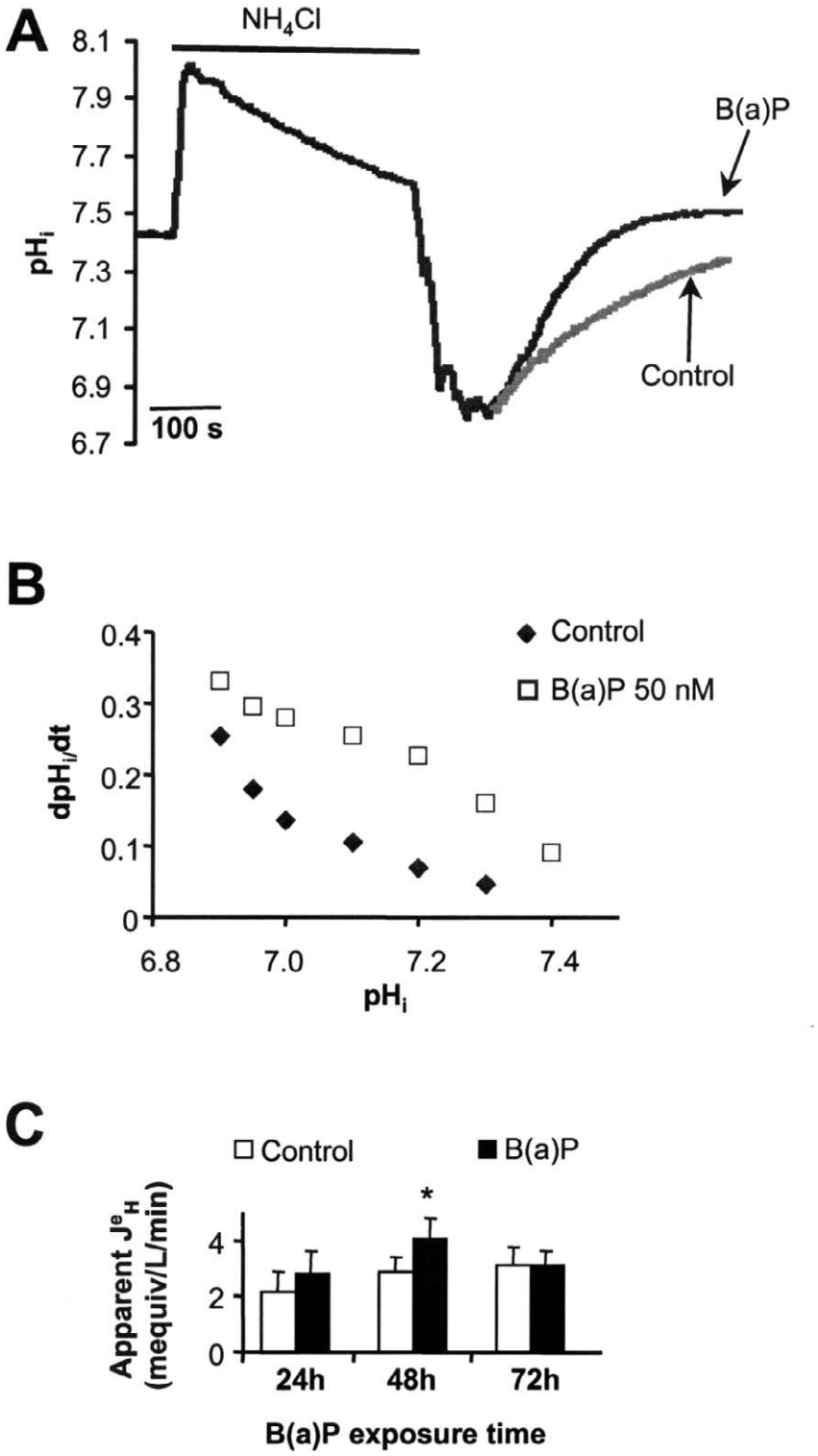

Figure 2. Determination of acid extrusion in cells treated with B(a)P. F258 cells were treated with 50 nM B(a)P for various exposure times. Subsequently, pH_i recovery rate was monitored following an acid load induced upon removal of NH_4Cl (20 mM) from extracellular medium (see Materials and Methods). ***A)*** Example of pH_i-recovery recording in both untreated and treated cells during 48 h. Only pH_i recovery recorded in control F258 cells is illustrated. ***B)*** Apparent dpH_i/dt (pH unit/min) estimated from the recordings illustrated in A. ***C)*** Mean apparent acid efflux J^e_H calculated from 4–10 independent experiments, at $pH_i = 6.9$ (see Materials and Method for calculation). *$P < 0.05$ treated vs. control.

Fig. 3

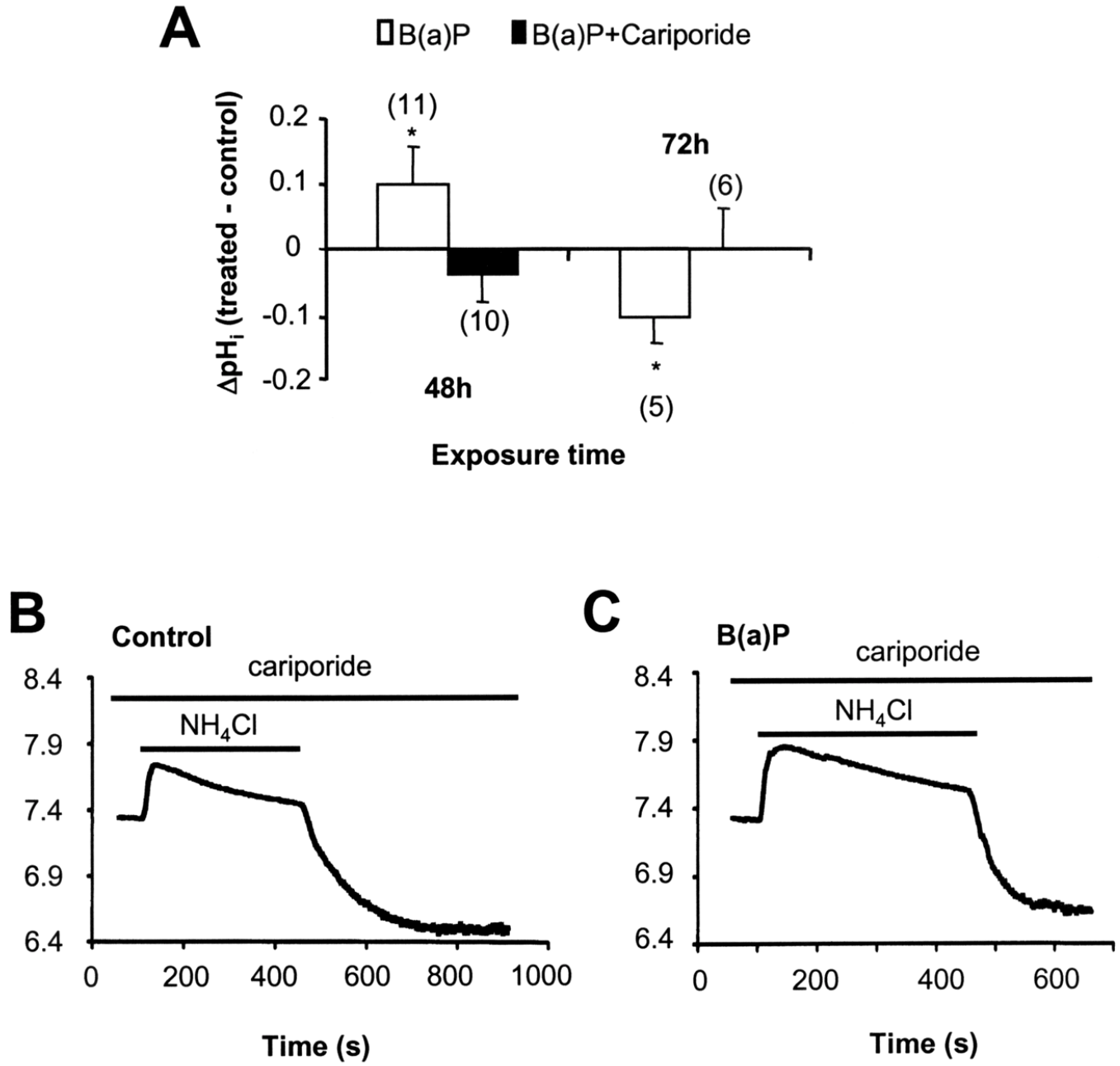

Figure 3. Effects of the NHE1-inhibitor, cariporide, on resting pH_i and on pH_i recovery in B(a)P-treated cells. ***A)*** Resting pH_i measurements recorded in F258 cells treated or not with B(a)P (50 nM) and/or cariporide (30 µM) for the times indicated in HEPES-buffered medium. Number in brackets given next to each bar represents the number of coverslips used (i.e., the number of performed measurements) from at least 3 independent experiments. Mean values correspond to the average of all pH_i determinations. Basal pH_i was 7.30 ± 0.04 (n=9) and 7.31 ± 0.03 (n=11) in control untreated and cariporide-treated cells, respectively. *P < 0.05 treated vs. control. ***B, C)*** Representative pH_i recordings from 12 independent experiments in cells treated with control + cariporide (***B***) and B(a)P + cariporide (***C***). Cells were superfused with HEPES-buffered medium with 30 µM cariporide and submitted to a NH_4^+ (20 mM) prepulse to activate acid extrusion.

Fig. 4

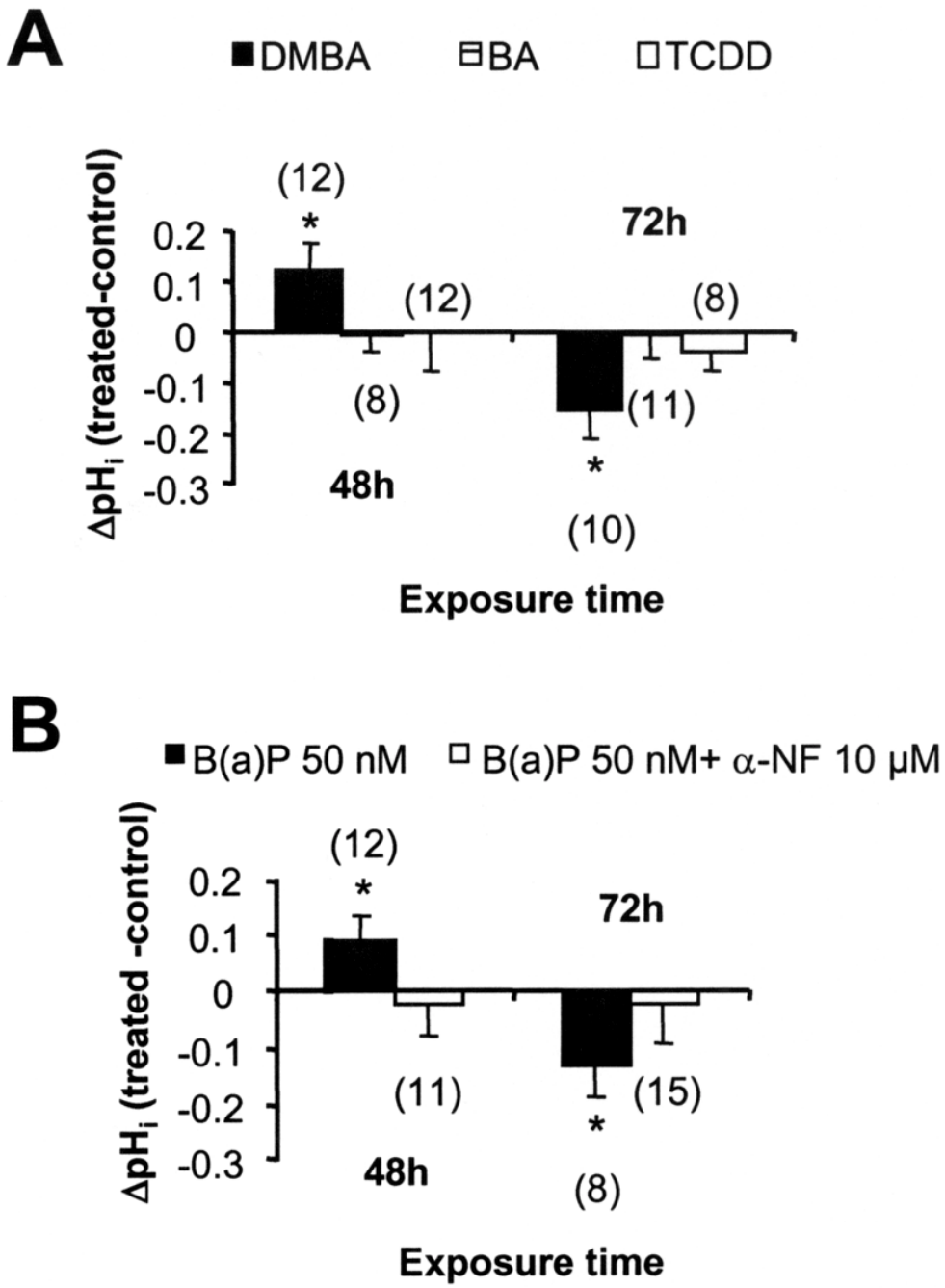

Figure 4. Role of CYP1A1-dependent metabolism of PAHs in pH_i variations. ***A)*** F258 cells were treated with either 50 nM DMBA or 50 nM BA (two PAHs), or a specific AhR-ligand, 50 nM TCDD, during 48 h and 72 h. ***B)*** F258 cells were cotreated with 50 nM B(a)P and 10 μM α-NF during 48 h and 72 h. Subsequently, resting pH_i was measured, and ΔpH_i between treated and control cells was calculated. Basal pH_i was 7.31 ± 0.04 (*n*=12) and 7.31 ± 0.03 (*n*=12) in control untreated and α-NF-treated cells, respectively. Number in brackets next to each bar represents the number of coverslips used (i.e., the number of performed measurements) from at least 3 independent experiments. Mean values correspond to the average of all pH_i determinations. **P* < 0.05 treated vs. control.

Fig. 5

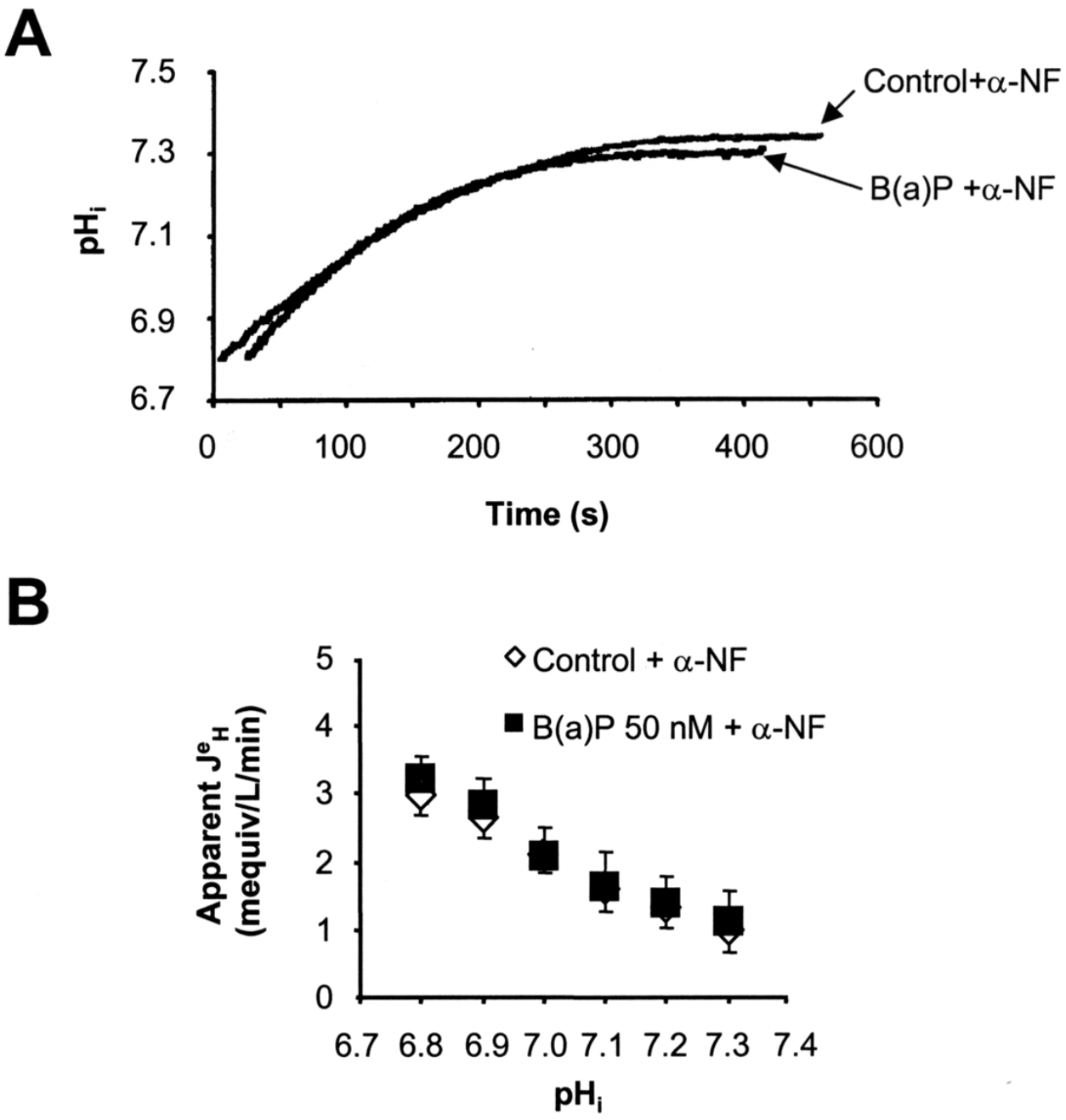

Figure 5. Effects of α-NF on the increase in acid extrusion elicited upon B(a)P. F258 cells were cotreated with 50 nM B(a)P and 10 µM α-NF for 48 h. pH_i recovery rate was monitored following an acid load induced upon NH_4Cl (20 mM) addition and subsequent removal. ***A)*** Recordings obtained from B(a)P + α-NF treated cells vs. control. ***B)*** Acid effluxes were calculated as described in Materials and Methods and averaged from 10 independent experiments.

Fig. 6

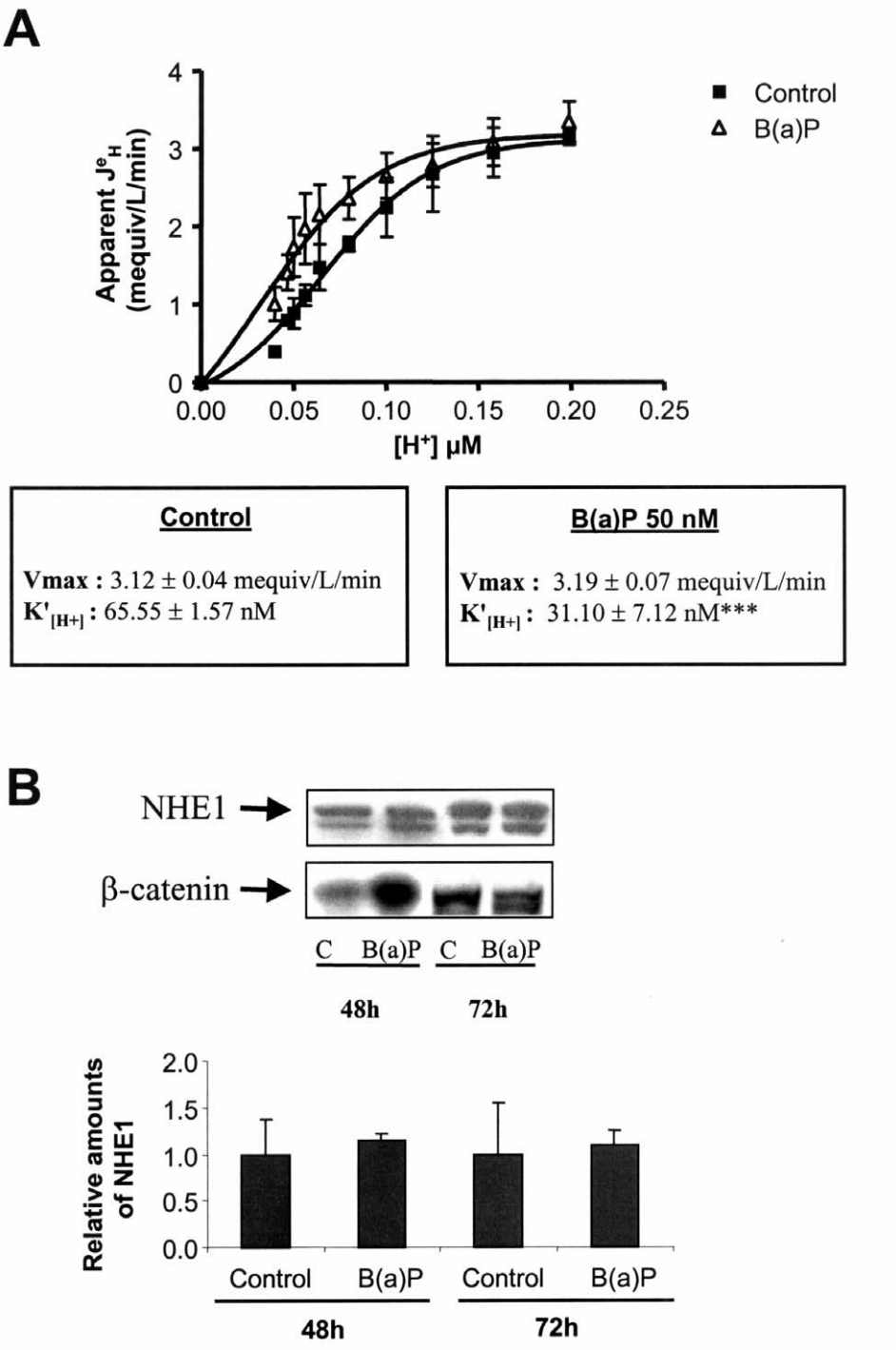

Figure 6. Kinetic analysis of NHE1 activity (*A*) and NHE1 protein expression (*B*) following B(a)P exposure of F258 cells. ***A)*** Treated and untreated F258 cells were acidified with NH_4Cl (20 mM) following a 48-h treatment with 50 nM of B(a)P. NHE1 efflux rates were calculated as described in Materials and Methods and averaged from 7 independent experiments. Curves were fitted to data by using a sigmoidal dose-response nonlinear regression. Kinetic parameters $K'_{[H+]}$ and V_{max} were estimated for control and B(a)P (50 nM)-treated F258 cells. ***$P < 0.001$, B(a)P vs. control. ***B)*** Western blot on membrane total proteins is performed with NHE1-specific antibody and β-catenin antibody (used as an invariant protein marker). Both the mature and the precursor forms of NHE1 are shown. The histogram showed the quantification of relative amounts of NHE1 protein. Results are expressed as means ± SE of 3 independent experiments, standardized by β-catenin and to respective controls.

Fig. 7

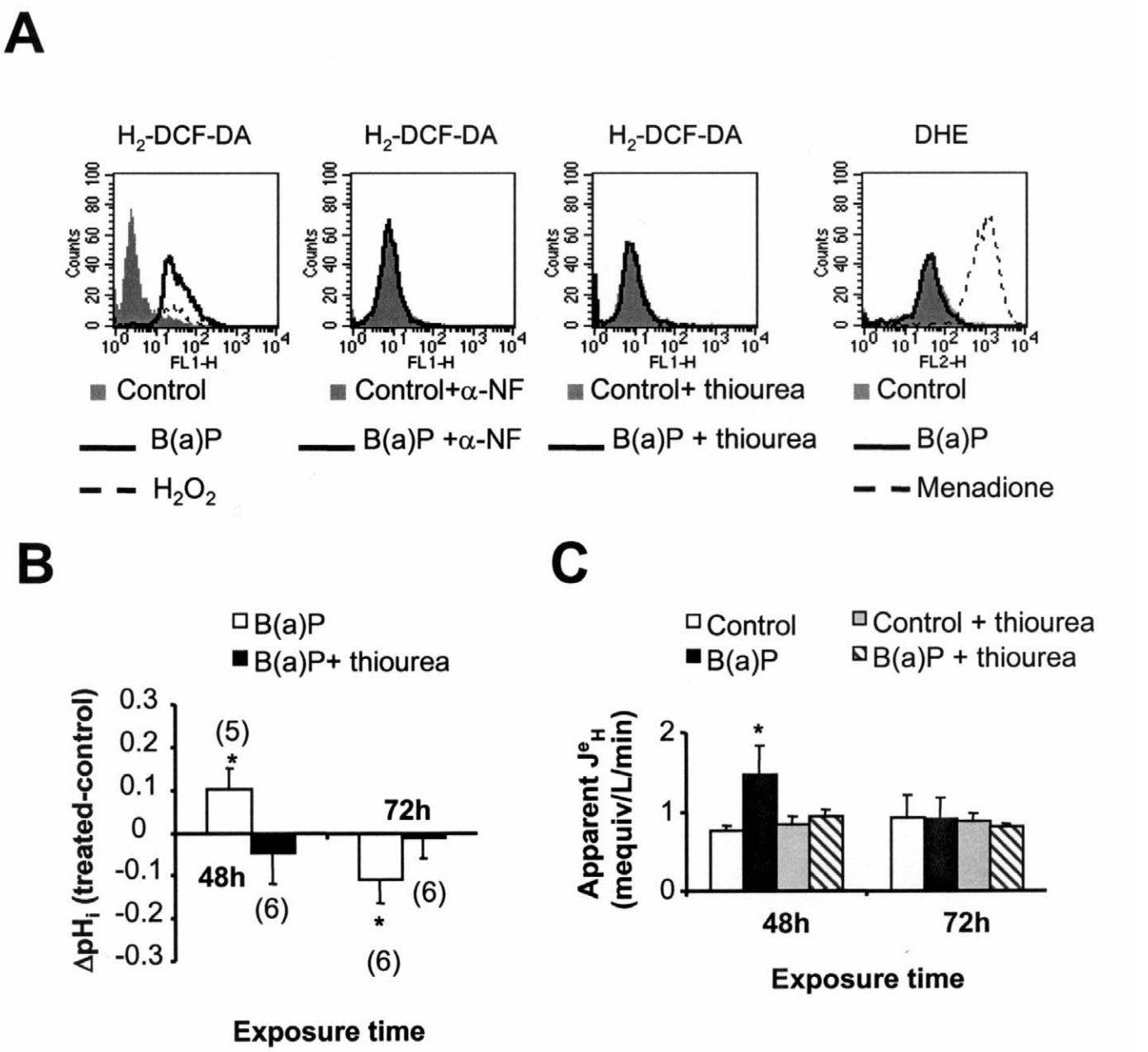

Figure 7. Involvement of CYP1A1-dependent ROS production in B(a)P-induced NHE1 activity. ***A)*** Production of ROS assessed by flow cytometry analysis. F258 cells were either untreated or treated with 50 nM B(a)P with or without a CYP1A1 inhibitor (10 μM α-NF) or an antioxidant (10 mM thiourea). H_2O_2 or $O_2^{-\cdot}$ were detected with H_2-DCF-DA or DHE probes, respectively. H_2O_2 (10 mM) and Menadione (100 μM) were used as positive control of H_2-DCF-DA or DHE probes, respectively. ***B)*** F258 cells were cotreated with 50 nM B(a)P and 10 mM thiourea, during 48 h and 72 h. Subsequently, resting pH_i was measured and ΔpH_i between treated and control cells was calculated. Basal pH_i was 7.37 ± 0.05 (n=6) and 7.39 ± 0.06 (n=9) in control untreated and thiourea-treated cells, respectively. Number in brackets next to each bar represents the number of coverslips used (i.e., the number of performed measurements) from at least 3 independent experiments. Mean values correspond to the average of all pH_i determinations. *$P < 0.05$ treated vs. control. ***C)*** F258 cells were cotreated with 50 nM B(a)P and 10 mM thiourea during 48 h. pH_i recovery rate was monitored following an acid load induced upon NH_4Cl (20 mM) addition and subsequent removal. Acid effluxes were calculated as described in Materials and Methods and averaged from 8 independent experiments. *$P < 0.05$, B(a)P-treated vs. control.

Fig. 8

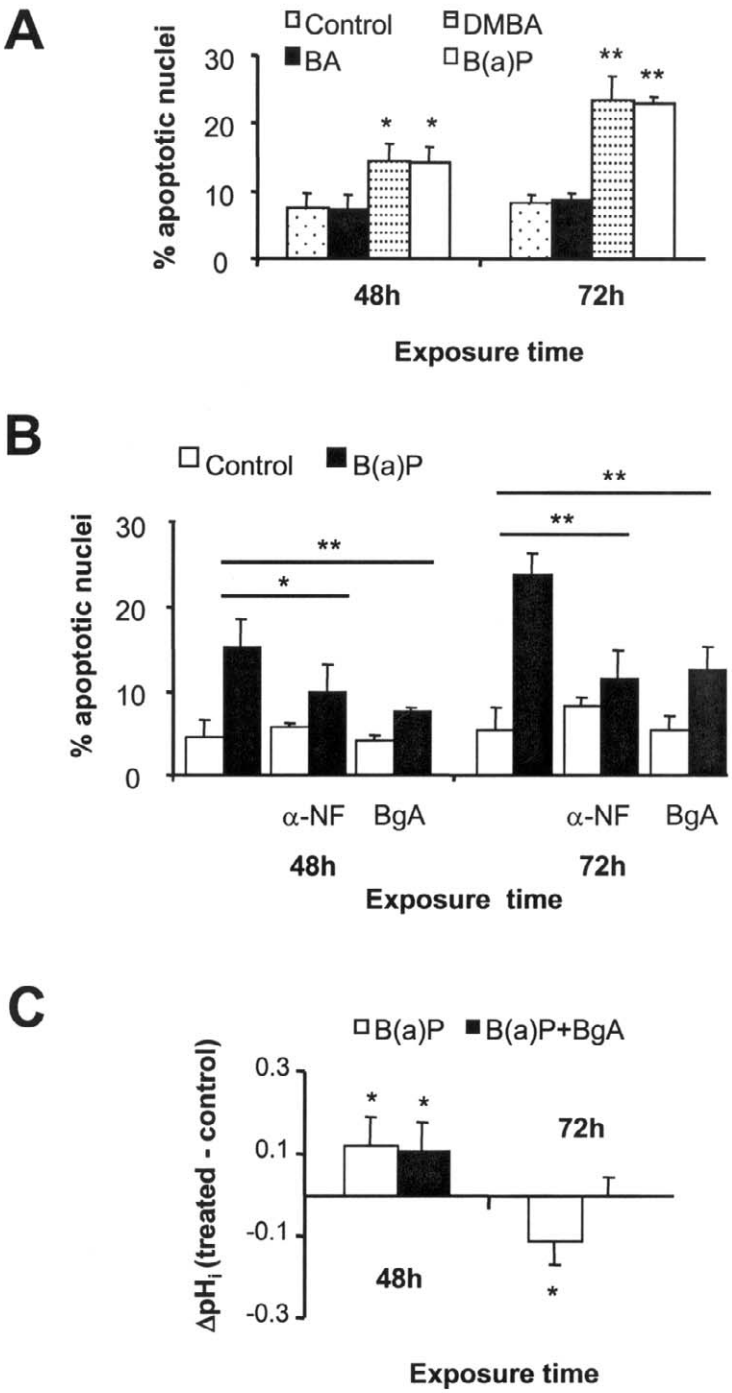

Figure 8. Role of metabolites and mitochondrial targeting in PAH-induced toxicity. F258 cells were treated during 48 h and 72h, subsequently collected, and stained with Hoechst 33342. Chromatin fragmentation and condensation were analyzed with a fluorescent microscope. ***A)*** Treatments with 50 nM BA, DMBA, or B(a)P **P* < 0.05, ***P* < 0.01 treated vs. control (*n*=6). ***B)*** Cotreatments with 50 nM B(a)P and 10 µM α-NF or 10 µM Bongkrekic acid (BgA). **P* < 0.05, cotreated B(a)P vs. control B(a)P (n=5). ***C)*** Resting pH_i was measured in B(a)P + BgA treated cells. Mean values correspond to the average of all pH_i determinations (*n*=9 performed measurements from at least 3 independent experiments). pH_i was 7.40 ± 0.05 (*n*=7) and 7.44 ± 0.03 (*n*=9) in control untreated and BgA-treated cells, respectively. **P* < 0.05, ***P* < 0.01 treated vs. appropriate control.

Fig. 9

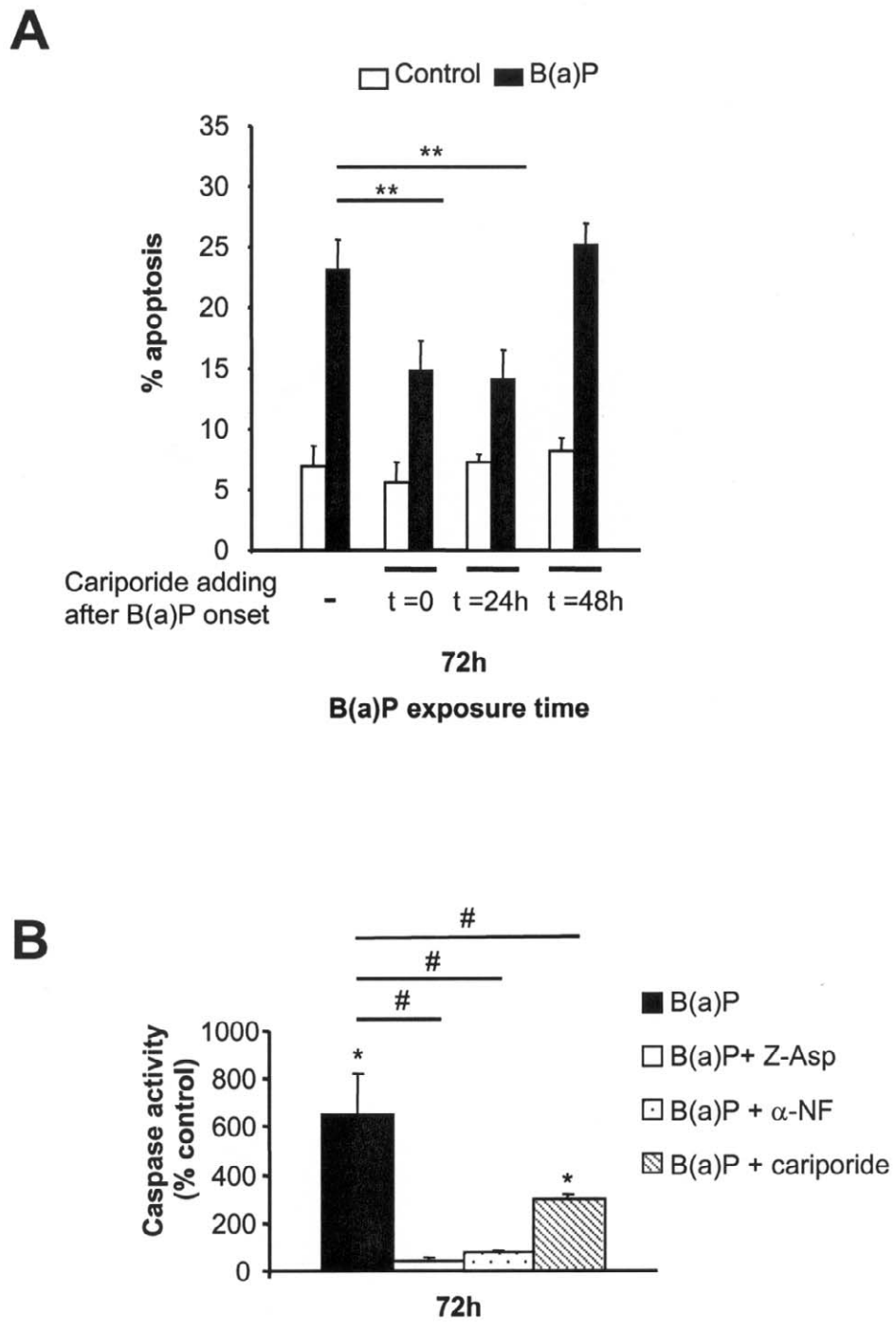

Figure 9. Role of NHE1 activation in PAH- induced toxicity. ***A)*** F258 cells were treated with 50 nM B(a)P alone or in the presence of 30 µM cariporide added at 0, 24, or 48 h after the onset of B(a)P treatment. Treatments with B(a)P were performed during 72 h. Subsequently, apoptotic nuclei were analyzed by Hoechst 33342 staining. **P* < 0.05, ***P* < 0.01, cariporide and PAH-treated cells vs. control PAH-treated cells (*n*=7 independent experiments). ***B)*** F258 cells were treated with 50 nM B(a)P alone or in the presence of 30 µM cariporide, 10 µM α-NF or 10 µM Z-Asp (a global caspase inhibitor). After a 72-h treatment, cells were harvested and washed with phosphate-buffered saline, before being lysed as described in Materials and Methods. Caspase activities (as detected by cleavage of DEVD-AMC) were measured by spectrofluorimetry and averaged from 5 independent experiments. **P* < 0.05, B(a)P ± inhibitor vs. control ± inhibitor; $^{\#}P$<0.05 B(a)P + inhibitor vs. B(a)P-treated cells.

Fig. 10

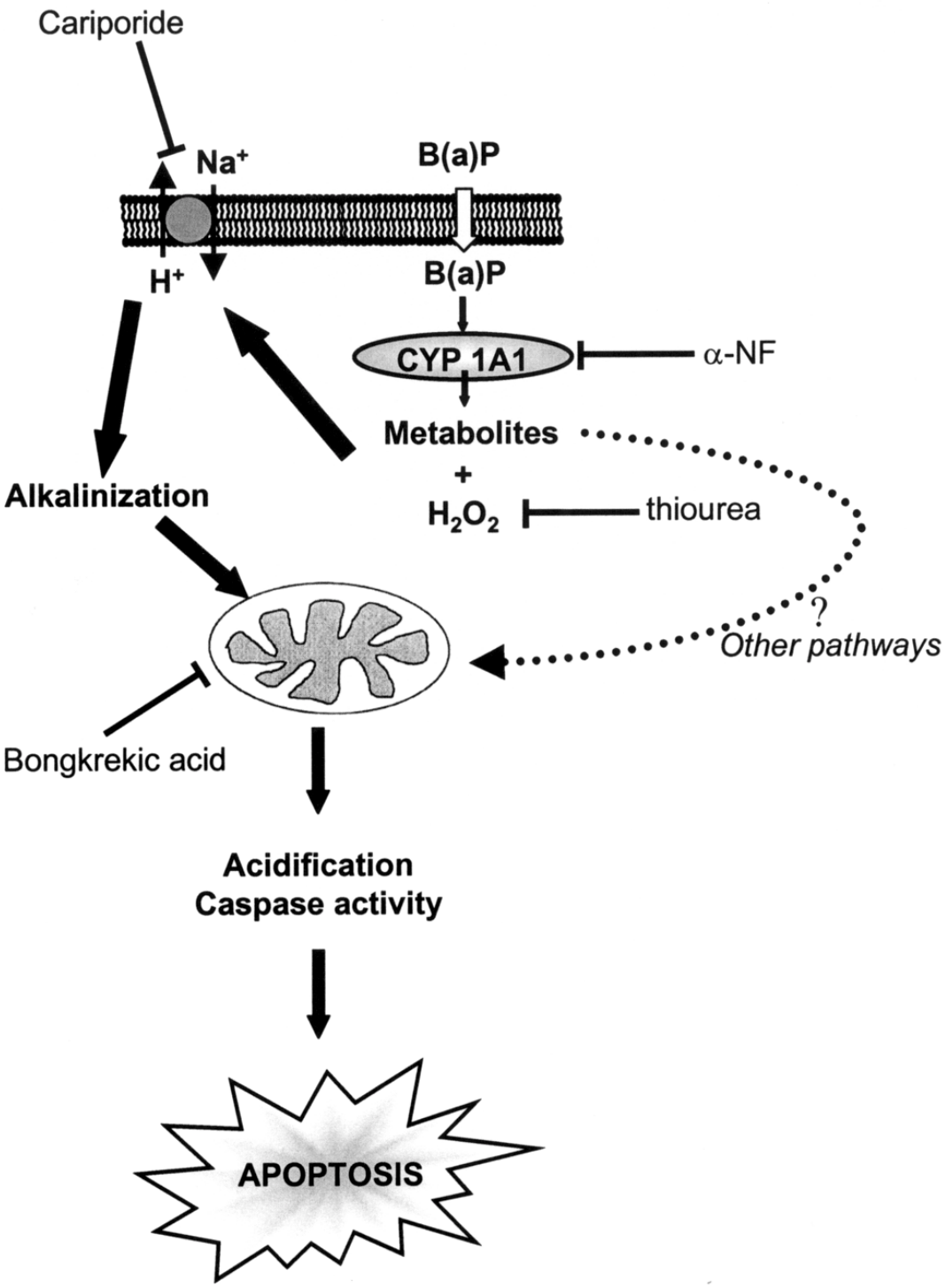

Figure 10. Recapitulative model of NHE1-dependent, B(a)P-induced apoptosis. B(a)P, a lipophilic molecule, goes across the bilayer membrane. In the cytosol, B(a)P is metabolized by CYP1A1 into reactive metabolites, which target NHE1 *via* H_2O_2 production, inducing an alkalinization. This activation favors the apoptotic signaling *via* mitochondria, leading to a late acidification and caspase activity corresponding to the effector phase of apoptosis. Other pathways (such as the p53 pathway) are likely to be involved in this model and are represented by a dotted arrow.